39Ar - 40Ar investigations within the Grande-Kabylie massif (northern Algeria) : evidences for its Alpine structuration

Autor(en): **Monié, Patrick / Caby, Renaud / Maluski, Henri**

Objekttyp: **Article**

Zeitschrift: **Eclogae Geologicae Helvetiae**

Band (Jahr): **77 (1984)**

Heft 1

PDF erstellt am: **25.09.2024**

Persistenter Link: https://doi.org/10.5169/seals-165501

Eclogae geol. Helv.	Vol. 77	Nr. 1	Pages 115–141	Basle, april 1984

^{39}Ar–^{40}Ar investigations within the Grande-Kabylie massif (northern Algeria): evidences for its Alpine structuration

By PATRICK MONIÉ[1]), RENAUD CABY[2]) and HENRI MALUSKI[1])

ABSTRACT

Within the Grande-Kabylie and Algiers massifs (northern Algeria), the tectonometamorphic structuration of the Kabyle basement has been investigated by the ^{39}Ar–^{40}Ar step degassing technique in a preliminary attempt to date the major metamorphic events structurally and petrographically identified.

An eo-Alpine age (85–95 m.y.) is suggested for the high-temperature regional metamorphism, generally considered to be Precambrian or Paleozoic.

In Grande-Kabylie, a major blastomylonitic event restricted to the Djebel Sidi Ali bou Nab area has affected a Hercynian granite and its country rocks. On a N–S cross section, two main tectonometamorphic episodes have been evidenced:

— a prograde synkinematic metamorphism with a N–S gradient, related to the motion of the blastomylonitic belt as a dextral low-dipping wrench fault;

— a tenuous second low-grade retrogression associated with late movements on the fault and characterized by a strong metamorphic inversion.

^{39}Ar–^{40}Ar data on synkinematic micas have yielded ages of 25 ± 1 m.y. for the high-grade blastomylonitic rocks; the age of the latter thrustings is not rigorously established.

A prekinematic muscovite displays an apparent age spectrum which does fit in with the usual behaviour of mineral systems which have undergone a polyphase evolution. This result is discussed in the light of deformation, recrystallization and temperature parameters.

RÉSUMÉ

Une étude structurale et pétrographique menée en Grande-Kabylie et dans le massif d'Alger (Algérie septentrionale) a permis la reconnaissance de diverses étapes majeures dans la structuration tectonométamorphique du socle Kabyle. La datation des principaux événements métamorphiques a été réalisée par la méthode ^{39}Ar–^{40}Ar en paliers croissants de température.

Le métamorphisme régional de haute température, jusqu'alors considéré d'âge Paléozoïque ou Précambrien, apparaît être d'âge éo-Alpin (85–95 Ma).

En Grande-Kabylie, une importante phase blastomylonitique limitée à la zone du Djebel Sidi Ali bou Nab a affecté un granite Hercynien et son encaissant. Les caractères tectonométamorphiques mis en évidence sur une coupe N–S nous ont amené à distinguer:

— un métamorphisme syncinématique prograde à gradient N–S, contemporain du fonctionnement en décrochement dextre de la zone blastomylonitique faiblement inclinée;

— un métamorphisme rétrograde tardif, peu développé, associé à une reprise à froid de la base des blastomylonites et souligné par une forte inversion métamorphique.

[1]) Laboratoire de Géologie Structurale, LA 266, U.S.T.L., place E. Bataillon, F–34060 Montpellier Cedex.
[2]) Centre Géologique et Géophysique, U.S.T.L., place E. Bataillon, F–34060 Montpellier Cedex.

La datation ^{39}Ar–^{40}Ar des micas syncinématiques permet d'attribuer un âge Oligo-Miocène (25 ± 1 Ma) à la phase blastomylonitique sans que l'âge des chevauchements tardifs ne puisse être rigoureusement établi.

Le spectre d'âge obtenu sur des muscovites primaires de pegmatites ne paraît pas traduire l'évolution polyphasée de ces minéraux. L'influence des paramètres déformation-recristallisation et température sur le comportement rétentif de ces micas est discutée.

Introduction

In northern Algeria, the Maghrebide Mountain Chain of Alpine age s.l. consists of several tectonic units of variable metamorphic grade and compositional character, separated by a series of E–W trending tectonic structures (Fig. 1). Descriptions of general relationships in this area may be found in DURAND-DELGA (1955, 1969), MATTAUER (1963), BOUILLIN (1977), GÉLARD (1979), VILA (1980) and BOSSIÈRE (1980).

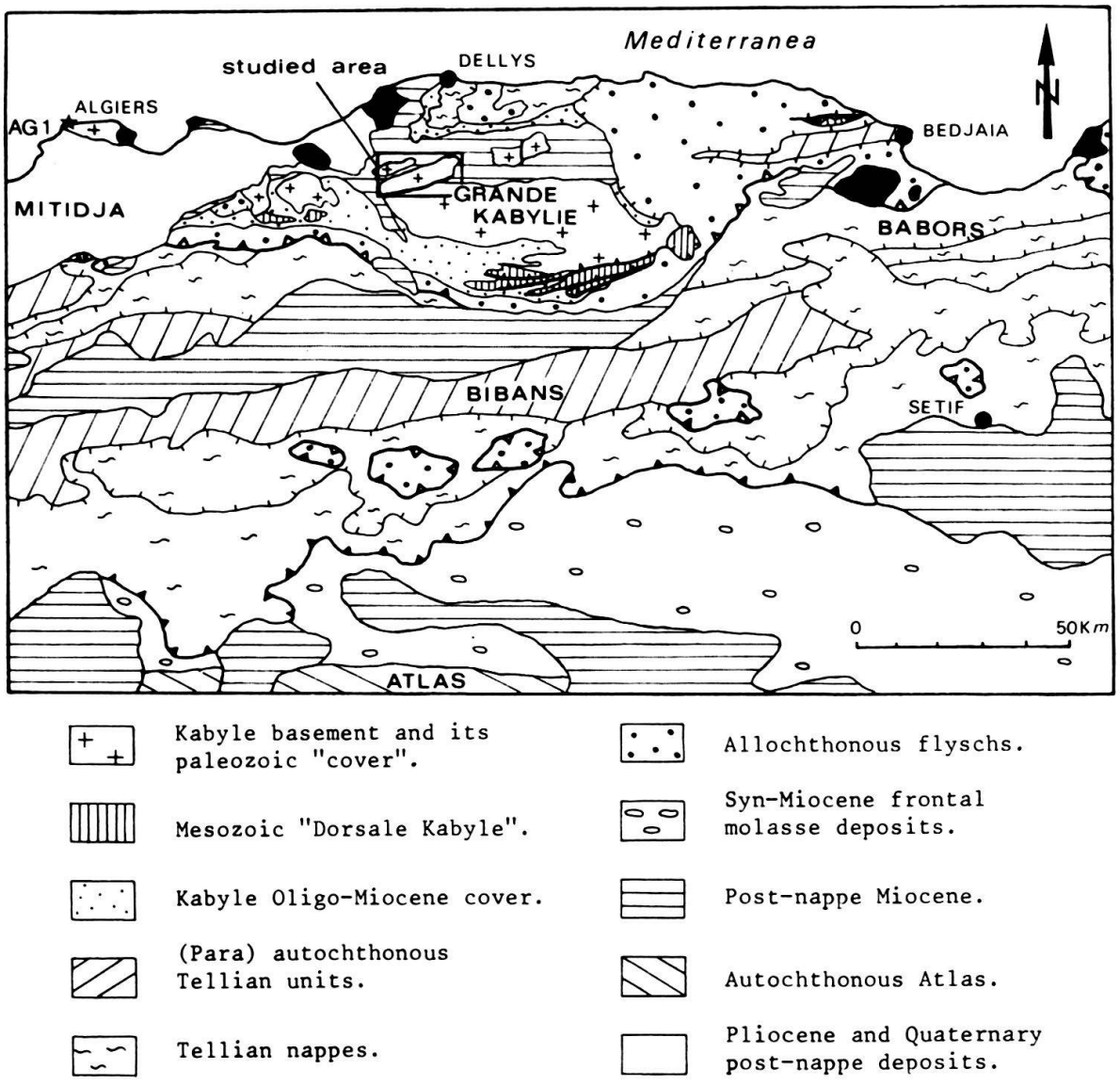

Fig. 1. Sketch map of the North African Chain in Algeria (after DEVAUX 1969, CAIRE 1975, RAYMOND 1976, WILDI 1983). Sample AG 1 from the Algiers massif is located.

East of Algiers, on a N–S section three main tectonic units can be discerned from the north to the south: 1. The inner crystalline basement of Grande-Kabylie which is constituted by two tectonic subunits separated by the ENE–WSW Sidi Ali bou Nab blastomylonitic belt (BOSSIÈRE 1977). Structural relationships with the overlying Paleozoic and Mesocainozoic sedimentary sequences are not clearly defined (BOSSIÈRE 1980). 2. The external domain or Tellian zones, extending north to the Atlas domain, is constituted by a complex stacking of nappes of Mesozoic pelites and limestones; autochthonous and low-grade terrains, deformed during a mid-Cretaceous event, appear in windows through the northern Tellian zones (BLÈS 1971; LEPVRIER 1971; OBERT 1974; BLANC & OBERT 1974). 3. Cretaceous and early-Tertiary flyschs which occur in allochthonous position above the internal and external domains. Their paleogeographic location and structural evolution are still discussed. For more details about the geology of the North African orogenic belt, the reader is referred to the recent compilation of WILDI (1983).

Until now, the tectonometamorphic evolution of the Grande-Kabylie basement has been interpreted in terms of two major events, a Pan-African orogenic episode during which the inner zones have been affected by a high-temperature regional metamorphism, and a Hercynian high-grade blastomylonitic event, localized to the Sidi Ali bou Nab shear zone (PEUCAT & BOSSIÈRE 1978, 1981).

In Petite-Kabylie, the Alpine orogeny resulted in a Eocene to Miocene southward overthrusting of the Kabyle basement onto the Tellian zones (DURAND-DELGA 1955; RAOULT 1974; BOUILLIN 1977); under the inner zones which were transported at least 40 km southward, the external Mesozoic series have been metamorphosed in greenschist facies. According to previous works, no significant Alpine metamorphism may have taken place within the Kabyle basement. However, from recent structural investigations in the Algiers and Grande-Kabylie massifs (MAHDJOUB 1981, SAADALLAH 1980, CABY 1982), an Alpine age has been suggested for the high-temperature regional metamorphism and the major shear zones activity. Moreover, PEUCAT & BOSSIÈRE (1981) gave Rb–Sr ages on biotites which may be correlated with a rejuvenation of the Kabyle basement by distinct Alpine thermal events. As ^{39}Ar–^{40}Ar method is a useful dating technique in polymetamorphic areas, we have carried out experiments on the more geologically significant samples we found in Grande-Kabylie, combined with a preliminary structural study.

I. Metamorphism and previous geochronology in the inner Maghrebide Chain

Since previous works of DURAND-DELGA (1951) in Petite-Kabylie, the regional metamorphism within the internal massifs is considered to be Pan-African or Caledonian in age. In Grande-Kabylie, to the top of a chlorite–biotite bearing schist series, the occurrence of late Cambrian pelites and sandstones (BAUDELOT & GÉRY 1979) would provide an upper limit to the age of this metamorphism. However, the stratigraphic position of this cover on the Kabyle basement is still somewhat uncertain. The contact between the two units is commonly underlined by a crushed zone, with an incipient cleavage and low-grade mineral associations (BOUILLIN 1977, BOSSIÈRE 1980), which could be interpreted as the base of a nappe. Therefore, assuming an allochthonous

position for the sedimentary cover, the age of the high-temperature metamorphism and deformation within the inner domain cannot be stratigraphically established.

Recently, PEUCAT & BOSSIÈRE (1978, 1981) reported different Rb–Sr whole-rock isochron and mineral ages which yielded fundamental results regarding the tectonic and thermal evolution of this area. Their whole-rock radiometric study has concerned the age of the Sidi Ali bou Nab granite (279 ± 8 m.y.) which outcrops in the blastomylonitic zone (Fig. 4), and the age of the high temperature metamorphic rocks, including 563 ± 24 m.y. and 465 ± 26 m.y. dates for the orthogneisses. The authors consider the age of the Sidi Ali bou Nab granite as the younger limit of the blastomylonitic event which acted upon the area where occurred the intrusion of this granite. The Rb–Sr biotites apparent ages in the orthogneisses and in the overprinted granite of Sidi Ali bou Nab range between 127–71 m.y. and 38–22 m.y. respectively, while the white micas exhibit more scattered values between 260 and 170 m.y.

PEUCAT & BOSSIÈRE have argued that the biotite dates result from different Alpine thermal rejuvenations of the Kabyle basement without apparent metamorphic recrystallizations. However, in the light of the typical behaviour of mineral Rb–Sr systems in polycyclic areas (for example the inner parts of the Western Alps – FREY et al. 1976), we suggest that the biotites ages point out different phases of Alpine metamorphism. In Petite-Kabylie, these events were bounded by a postkinematic magmatism of Miocene age (BELLON 1976).

At the northern boundary of the external domain, various structural and paleontological data point out to a Cretaceous age for the low-grade metamorphism and E–W trending penetrative deformation which affected the autochthonous Tellian zones (LEPVRIER 1971, OBERT 1974). In the Zaccar massif, a preliminary ^{39}Ar–^{40}Ar determination on chlorite at 85 ± 8 m.y. has been correlated with this Cretaceous event (MALUSKI et al. 1978), although this mineral has been shown to be poorly adequate to ^{39}Ar–^{40}Ar dating because of its high H_2O content.

Reviewing all the stratigraphic, structural and radiometric data, we found no decisive argument to rule out this Alpine interpretation of the regional metamorphism. Moreover, such an Alpine age s.l. seems to be consistent with the geological setting of the inner Riffian zones (Morocco) where the granulite facies metamorphism of Beni Bousera is known to be 20–22 m.y. old (LOOMIS 1975, POLVÉ & ALLÈGRE 1982, MICHARD et al. 1983) and with the Alpine tectonometamorphic evolution of the Betic Cordilleras (PUGA 1977, TORRES-ROLDÁN 1979).

II. Experimental techniques

All micas separates used in this study were obtained using heavy liquid and magnetic separator techniques. Final purification is achieved with ultrasonic cleaning in ethanol. Purity of these mineral fractions, sized between 0.08 and 0.16 mm in diameter, was better than 99%. Five samples along with the interlaboratory standard MMHb 1 at 520 ± 5 m.y. (ALEXANDER et al. 1978) sealed under vacuum in quartz vials, have been irradiated for 24 hours in the Melusine reactor of CENG (Grenoble, France). The fast neutron flux was about $10^{13}/cm^2/s$ and we have verified that its gradient across the cannister was lower than three percent. After irradiation, the samples were wrapped in high purity nickel foils and loaded in the vacuum extraction system. All the samples are baked out during 24 hours at 180°C. Subsequent stepwise argon extractions from the irradiated samples were carried out in a Mo crucible using a radiofrequency generator. Samples were maintained for one hour at each temperature step during incremental heating except for the fusion which is only 30

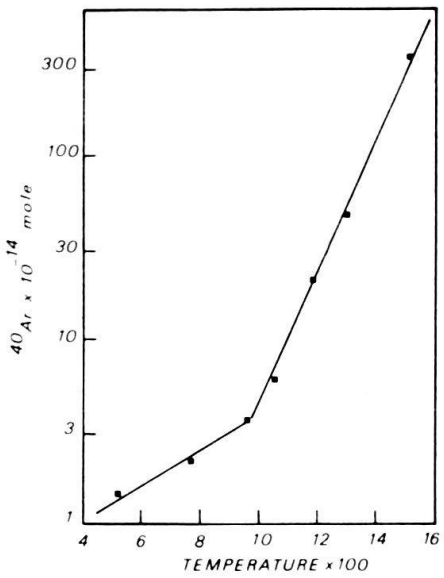

Fig. 2. ^{40}Ar release curve used for blank correction. ^{36}Ar blank corrections were carried out assuming a $^{40}Ar/^{36}Ar$ ratio of 295.5.

min in duration. High temperatures (> 750 °C) were monitored using an optical pyrometer and they are extrapolated to lower ones by plotting temperature against induction power. Uncertainty in these temperatures is about ± 15 °C.

The purification of the gas is achieved with a mixture of dry-ice and acetone and with Zr–Al getters at 400 °C. Argon is trapped on active charcoal fingers at liquid nitrogen temperature, then released into the mass spectrometer. Argon isotopic compositions were measured in the static mode. The data have been corrected for mass discrimination, irradiation masses interferences, radioactive decay of ^{37}Ar and blanks. To determine correction factors for interfering isotopes produced by nuclear reactions during irradiation, CaF_2 and K_2SO_4 pure salts have been analyzed. Factors a, b and c (BRERETON 1970) used to correct these effects are given in Table 1. Before analyzing each sample, we have run a series of blanks through the whole extraction-purification system at increasing temperature using the same incremental procedure as for a sample analysis. The release curve for ^{40}Ar (Fig. 2) shows that blank contribution is lower than 3×10^{-14} moles for temperatures up to 950 °C but for higher values, this contribution increases rapidly up to 3×10^{-12} moles at 1500 °C. Corrections were carried out assuming an atmospheric composition for blanks, which is only verified for the high-temperature steps.

Apparent $^{39}Ar/^{40}Ar$ ages were calculated from the corrected isotopic ratios (BRERETON 1970) using the recommended decay constants (STEIGER & JÄGER 1977). Uncertainty in each apparent age is given at two standard deviation (2 σ). $^{40}Ar/^{36}Ar$ vs $^{39}Ar/^{36}Ar$ isochrons have been computed with the data obtained from each sample using two-error regression method (YORK 1969). The mean square of the weighted deviates (MSWD) is used to statistically evaluate isochron definition and $^{40}Ar/^{36}Ar$ intercept.

The samples studied were selected as suitable representatives of the main tectonometamorphic episodes which affected the Kabyle basement; they were chosen to avoid as far as possible the effects of the intense meteoric alteration. ^{39}Ar–^{40}Ar incremental release ages have been determined for six micas concentrates separated from samples of paragneisses and leucosomes. The ^{39}Ar–^{40}Ar analytical data are listed in Table 1 and plotted as age spectra. Results for correlation isotopic diagrams $^{40}Ar/^{36}Ar$ vs $^{39}Ar/^{36}Ar$ are presented in Table 2.

III. The Algiers massif

The Algiers crystalline massif is regarded as an outlier of the Kabyle basement. This massif has been subdivided into six thin tectonic slices gently dipping south, which strongly differ in lithology and metamorphic grade (SAADALLAH 1981, 1982). They

Table 1: *^{39}Ar–^{40}Ar analytical data for incremental heating experiments. Ratios have been corrected for mass discrimination, decay, isotopes derived from interfering neutron reactions and blanks. Correction factors for interfering nuclear reactions are: $a = 0.202 \times 10^{-2}$; $b = 0.0216$; $c = 0.85 \times 10^{-3}$.*

T(°C)	40Ar*/39Ar	37Ar/39Ar	36Ar/39Ar	Cumulative 39Ar (%)	Age (Ma) +/- 2σ
Biotite AG1 (100-125 μ; 80.8 mg) J=0.012948					
1-390	4.349	-	0.18168	0.06	98.8 +/- 25.6
2-450	3.229	-	0.08225	0.18	73.9 11.9
3-520	3.203	-	0.02236	0.47	73.3 6.5
4-580	2.047	-	0.01272	1.35	47.2 3.8
5-640	2.729	-	0.00493	5.95	62.6 2.3
6-700	3.734	-	0.00168	22.42	85.2 2.1
7-755	3.914	-	0.00050	43.80	89.2 2.1
8-805	3.947	-	0.00101	55.24	89.9 2.1
9-860	3.626	-	0.00481	59.36	82.8 2.6
10-905	3.581	-	0.00896	61.83	81.8 3.5
11-960	3.635	-	0.00761	64.58	83.0 3.2
12-1005	3.644	0.0052	0.00730	68.49	83.2 3.2
13-1060	3.681	-	0.00583	74.51	84.0 2.9
14-1105	3.734	-	0.00053	79.05	85.2 2.0
15-1205	3.886	-	0.00013	90.50	88.6 2.0
16-1300	4.080	-	0.00044	99.79	92.6 2.1
17-1545	3.890	-	0.05368	100.	88.6 14.0
Total 39Ar = 2.8092 .10^{-11} mole Total age :85.9 +/- 2.2					
Muscovite AG1 (100-125 μ; 99.3 mg) J=0.012948					
1-390	0.729	-	0.07380	0.02	16.9 +/- 18.7
2-520	1.275	-	0.00900	0.47	29.5 2.6
3-580	1.312	0.0204	0.00466	1.22	30.4 1.6
4-640	1.798	0.0145	0.00359	2.59	41.5 1.6
5-700	2.071	0.0061	0.00309	5.16	47.7 1.6
6-755	2.839	0.0042	0.00220	9.27	65.1 1.8
7-805	3.249	0.0032	0.00108	17.27	74.3 1.8
8-805	3.632	0.0027	0.00118	21.68	82.9 2.0
9-860	3.552	-	0.00181	28.41	81.1 2.0
10-905	3.849	0.0014	0.00136	39.08	87.7 2.1
11-960	3.824	0.0009	0.01004	50.63	87.2 3.7
12-1005(1)	3.270	0.0015	0.02906	57.16	74.8 8.0
13-1060	3.938	0.0011	0.00276	64.67	89.7 2.4
14-1380(2)	4.188	-	0.00203	100.	95.3 2.4
Total 39Ar = 3.8298 .10^{-11} mole Total age :84.8 +/- 2.7					
Biotite KAB14 (80-125 μ; 130.4 mg) J=0.014232					
1-445	1.445	-	0.04242	0.09	36.7 +/- 12.1
2-525	0.488	-	0.01158	1.10	12.5 3.3
3-595	0.735	0.0158	0.00871	3.35	18.8 2.6
4-655	0.750	0.0088	0.00693	13.29	19.2 2.2
5-710	0.921	0.0076	0.00612	29.79	23.5 2.0
6-760	0.956	0.0064	0.00276	53.85	24.4 1.1
7-795	1.017	0.0052	0.00179	75.92	25.9 0.9
8-825	0.996	0.0062	0.00246	81.91	25.4 1.1
9-865	0.962	0.0111	0.00370	84.08	25.4 1.4
10-915	0.894	-	0.00461	85.51	22.8 1.6
11-985	0.984	0.0109	0.00288	90.69	25.1 1.2
12-1025	0.995	0.0098	0.00290	97.00	25.4 1.2
13-1055	0.905	0.0150	0.00466	99.58	23.1 1.6
14-1395	0.927	0.6031	0.01235	100.	23.6 3.7
Total 39Ar = 3.2725 .10^{-11} mole Total age :23.9 +/- 1.4					

T(°C)	40Ar*/39Ar	37Ar/39Ar	36Ar/39Ar	Cumulative 39Ar (%)	Age (Ma) +/- 2σ
Muscovite KAB14 (80-100 μ; 135 mg) J=0.014232					
1-445	0.762	-	0.02806	0.05	19.5 +/- 8.0
2-525	0.959	-	0.00316	0.46	24.5 1.2
3-595	1.017	-	0.00017	1.14	25.9 0.6
4-655	1.011	-	0.00087	2.24	25.8 0.7
5-710	0.900	-	0.00123	4.39	23.0 0.8
6-760	0.979	0.0581	0.00119	9.20	24.9 0.7
7-770	0.962	-	0.00072	12.77	24.5 0.6
8-825	0.996	-	0.00045	25.48	25.4 0.6
9-875	1.014	0.0110	0.00036	45.56	25.8 0.7
10-915	1.012	0.0476	0.00092	50.93	25.8 0.6
11-965	0.990	0.0328	0.00065	56.34	25.2 0.6
12-1010	1.014	0.0320	0.00063	61.82	25.8 0.6
13-1050	1.007	-	0.00034	73.00	25.7 0.6
14-1095	1.047	-	0.00025	90.01	26.7 0.6
15-1135	0.993	-	0.00043	99.36	25.3 0.6
16-1430	0.428	-	0.02160	100.	10.9 6.1
Total 39Ar = 3.5898 .10^{-11} mole Total age :25.6 +/- 0.7					
Muscovite KAB15-2 (80-100 μ; 123.4 mg) J=0.014232					
1-520	0.502	-	0.00512	0.18	12.8 +/- 1.6
2-595	0.954	-	0.00110	0.65	24.3 0.7
3-655	0.718	-	0.00210	1.22	18.3 0.9
4-710	0.981	0.0312	0.00052	3.61	25.0 0.6
5-760	0.960	0.0207	0.00039	6.33	24.5 0.6
6-795	0.977	0.0032	0.00023	16.15	24.9 0.6
7-825	0.973	0.0136	0.00028	23.28	24.8 0.6
8-865	0.965	0.0059	0.00029	35.22	24.6 0.6
9-915	0.964	0.0304	0.00043	38.04	24.6 0.6
10-950	0.942	0.0079	0.00033	47.11	24.0 0.6
11-985	0.962	-	0.00025	58.63	24.5 0.6
12-1025	0.992	-	0.00016	78.41	25.3 0.6
13-1055	0.981	-	0.00021	97.36	25.0 0.6
14-1100	0.972	-	0.00016	99.83	24.8 0.6
15-1315	0.658	-	0.01985	100.	16.8 5.7
Total 39Ar = 5.6052 .10^{-11} mole Total age :24.8 +/- 0.6					
Muscovite KAB15-1 (80-160 μ; 132.5 mg) J=0.014232					
1-525	2.679	-	0.02468	0.34	67.5 +/- 7.5
2-595	2.056	-	0.01500	0.72	52.0 4.8
3-655	2.427	-	0.00510	1.75	61.2 2.4
4-710	2.217	-	0.00253	3.82	56.0 1.7
5-760	2.332	-	0.00104	9.14	58.9 1.5
6-795	2.243	-	0.00118	17.26	56.7 1.5
7-825	2.280	0.0308	0.00119	20.72	57.6 1.5
8-710 (3)	2.287	-	0.00192	21.03	57.8 1.6
9-760	2.248	-	0.00103	22.06	56.8 1.4
10-795	2.225	-	0.00150	25.29	56.2 1.5
11-825	2.205	-	0.00194	30.21	55.8 1.6
12-875	2.251	0.0265	0.00310	34.85	56.9 1.8
13-915	2.253	0.0297	0.00298	38.68	56.9 1.8
14-950	2.251	-	0.00313	46.14	56.9 1.8
15-1130	2.205	-	0.00290	99.90	55.7 1.8
16-1165	2.579	-	0.01509	99.99	65.0 5.0
17-1395	2.564	-	0.34133	100.	64.6 93.8
Total 39Ar = 4.9722 .10^{-11} mole Total age :56.4 +/- 1.7					

Table 2: *Isochron data calculated with two-error regression method* (YORK 1969).

Sample	Total-gas data			Plateau data		
	Isochron age	$^{40}Ar/^{36}Ar$ intercept	MSWD	Isochron age	$^{40}Ar/^{36}Ar$ intercept	MSWD[1]
Biotite AG 1	88.9 ± 1	112 ± 3	> 100	85.3 ± 0.8	283 ± 6	0.42[2]
Muscovite AG 1	86 ± 4.7	70 ± 3	> 100	-	-	-
Biotie KAB 14	27.3 ± 0.5	259 ± 6	0.74	26.8 ± 0.5	270 ± 11	0.35
Muscovite KAB 14	26.3 ± 0.2	254 ± 10	0.91	26.3 ± 0.3	234.5 ± 23	0.84
Muscovite KAB 15.1	57.2 ± 0.5	286 ± 7	1.18	57.2 ± 0.5	283 ± 11	0.69
Muscovite KAB 15.2	25.1 ± 0.6	140.7 ± 26	10.87	25 ± 0.8	223 ± 67	2.48

[1] Mean square of the weighted deviates
[2] Calculed with steps 6, 9-14, 17.

include greenschists to the top and micaschists, gneisses of lower amphibolite facies grade below (Unit IV), slices of various orthogneisses and a lower unit of retrogressed garnetiferous schists. Slightly dipping bands of ultramylonites and cataclasites cross-cut the tectonic pile, which, according to the abrupt change in metamorphic grade between different units, may have formed during a late Alpine event long after the high-temperature metamorphism well preserved in unit IV. MAHDJOUB (1981, 1982) studying the petrofabric of orthogneisses and high-grade metamorphic rocks has shown the synkinematic metamorphism affecting the various gneisses of the lower units with overall E–W horizontal stretching lineations to have undergone the same syn-metamorphic deformation with a subhorizontal foliation. The microstructural and petrofabric data point to a simple shear regime with eastward horizontal movements.

Age of the high-temperature regional metamorphism

In order to date the high-temperature metamorphism which entirely affects unit IV and on which part of Algiers is built, we have selected a paragneiss sample of amphibolite facies from the Cap Caxine (Fig. 1). This unit is characterized by a syn- to late-kinematic mineral association with quartz + oligoclase + biotite + sillimanite + garnet (± muscovite ± K-feldspar + cordierite). The late poekilitic muscovite forms also cross-cutting veinlets of pneumatolytic origin, in connection with cordierite and mica-rich patches and tourmaline-bearing pegmatites. Muscovite and reddish-brown biotite in polygonal arcs of late microfolds appear to have crystallized during and in a late stage of deformation. Later kinking and incipient chloritization of the biotite may

---

[1]) Heating step with a great experimental air contamination.
[2]) Due to analytical problems, the fusion data had not been published in the first short paper.
[3]) From step 8 to 14, the temperature variations are due to HF heater unstability.
$^{40}Ar^*$ refers to radiogenic argon.

reflect younger movements in connection with the low dipping zones of ultramylonite, cataclasite and pseudotachylyte described in this unit (SAADALLAH 1981).

^{39}Ar–^{40}Ar incremental-release heating experiments have been carried out on coexisting biotite and muscovite from this sample. The data have been previously published in a short paper (MONIÉ et al. 1982) and we remind here the main conclusions suggested by these results. Both age spectra obtained on biotite and muscovite AG 1 (Fig. 3) are characteristic of isotopic systems which have suffered a partial argon loss subsequent to their closure (BERGER 1975, HANSON et al. 1975, ALBARÈDE et al. 1978, MALUSKI 1978, DALLMEYER 1982). The apparent age spectrum for muscovite conforms with diffusion models predicted by TURNER (1968) and HARRISON & MC DOUGALL (1980). Low temperature increments yield minimum ages around 30 ± 2 m.y. which are regarded as a maximum age for the later retrogression superposed on the amphibolite facies paragenesis. This later event is correlated with the activity of low-grade shear zones bearing chlorite assemblages. On the other hand, AG 1 muscovite releases most of its ^{39}Ar (65%) in the high-temperature steps which display a total age at 92.5 ± 2.6 m.y. The apparent age spectrum for the coexisting biotites defines a trend, with a saddle-shaped profile, for over 94% of the ^{39}Ar released. These gas fractions correspond to a total age of 87.4 ± 2.2 m.y., consistent with the above data obtained on muscovite. In addition to the saddle-shaped pattern, a low temperature trough at 47.2 ± 3.8 m.y. in step 4 followed by a progressive increase in ages may give evidence for a minor resetting of the mineral subsequent to its growth. Thus, the age spectra of both minerals appear to reflect two thermal events which may be correlated with the tectonic and metamorphic history of the Kabyle basement. The ^{39}Ar–^{40}Ar data suggest an age of 85–95 m.y. for the high-temperature regional metamorphism, concordant with the Rb–Sr biotite ages of 71–95 m.y. displayed by the gneissic rocks of the Grande-Kabylie massif (PEUCAT & BOSSIÈRE 1981). We found also consistency with the ^{39}Ar–^{40}Ar age on chlorite at 85 ± 8 m.y. related to a regional low-grade metamorphism in the external domain (MALUSKI et al. 1978).

The younger ages obtained from the less retentive sites, respectively 47.2 ± 3.8 m.y. for the biotite and 30 ± 2 m.y. for the muscovite, are thought to represent the reactiva-

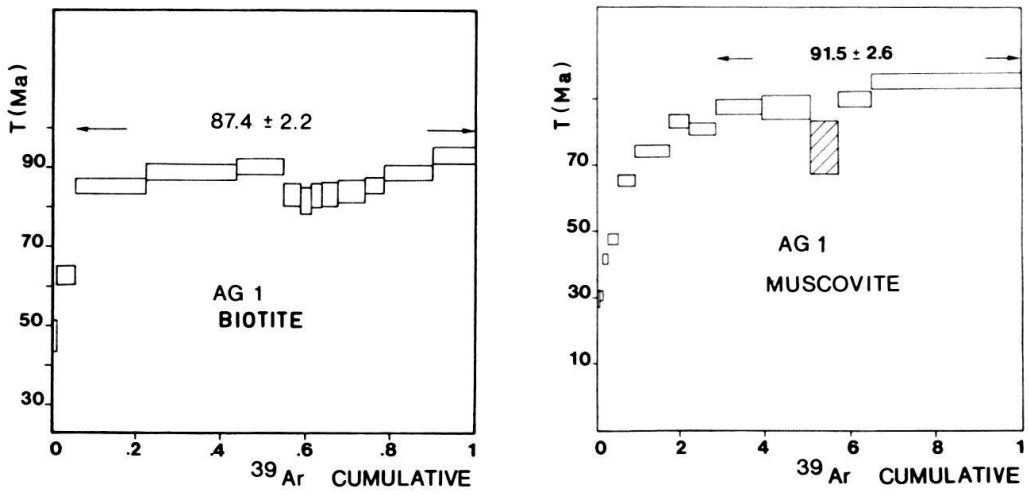

Fig. 3. Apparent age spectra of biotite (a) and muscovite (b) from the Algiers massif paragneisses.

tion of mineral systems associated with the later deformation under low-grade metamorphic conditions. An upper limit at 30 ± 2 m.y. may be attributed to this high-level tectonic event during which the different units were pilled up and the retrogressive mylonites generated.

IV. The Grande-Kabylie massif (Fig. 4)

Petrographic studies on this massif have allowed to BOSSIÈRE (1980) a tentative distinction of a gneiss-marble "basement" and phyllite "cover", both units being partly involved in a ENE–WSW high strained blastomylonitic zone within which the Sidi Ali bou Nab granite (further noticed SAN granite) was intruded. Brief structural observations concerning the geometry and kinematics of this blastomylonitic zone are re-

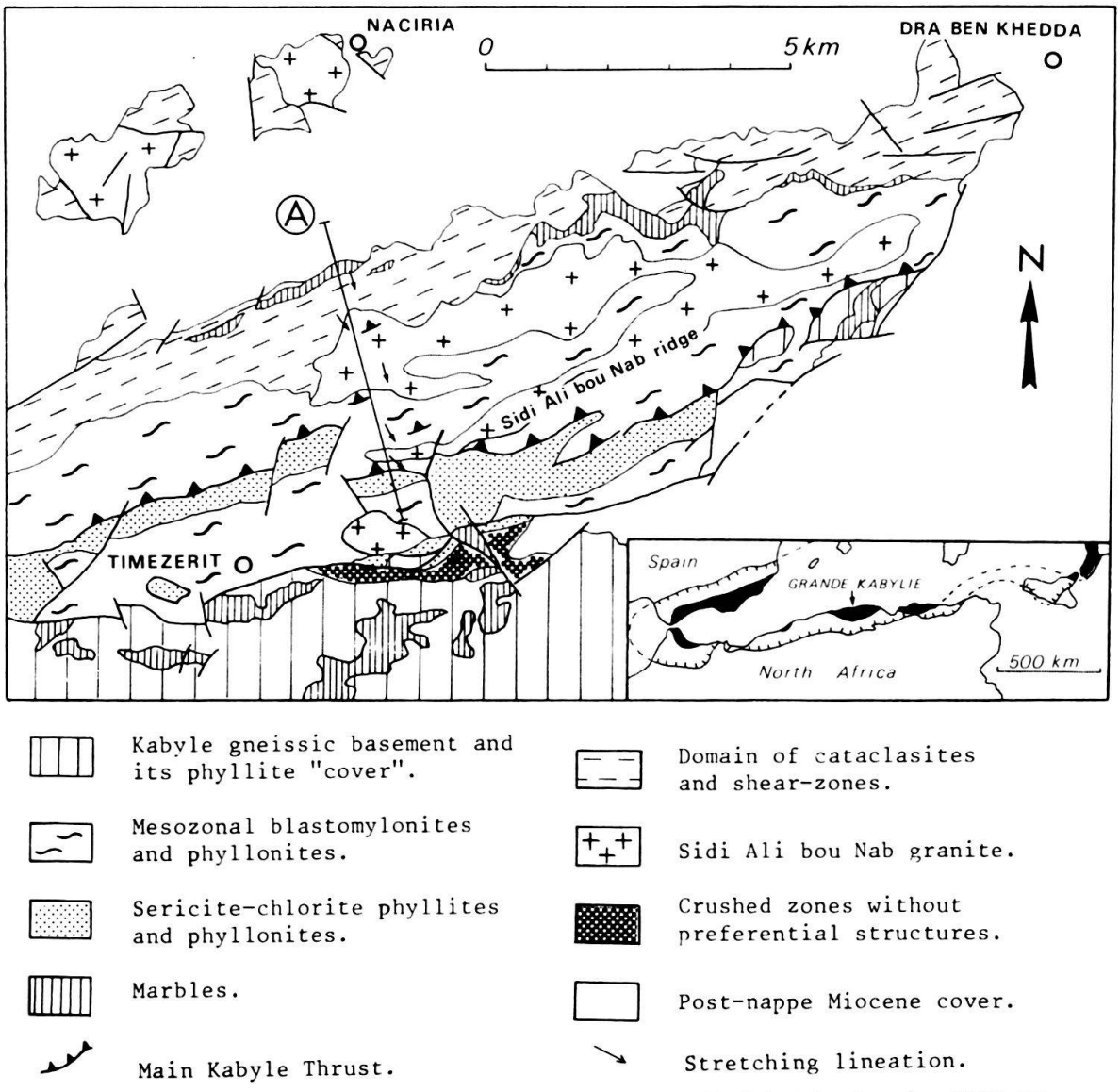

Fig. 4. Structural subdivisions of the Sidi Ali bou Nab blastomylonitic belt (after BOSSIÈRE 1980). The cross section of Figure 5 is also located. Inset: Situation of the Grande-Kabylie massif within the Alpine orogen of western Mediterranea.

ported below. They significantly differ from the interpretation proposed by BOSSIÈRE (1975, 1980) though many of its partial conclusions based on very pertinent petrographic observations are not revised.

From a purely structural point of view, we can divide on a N–S section this crystalline massif into four zones in which we recognize a progressive evolution of the deformation and metamorphism with a N–S gradient across the SAN ridge, thrusted upon lower grade phyllites (Fig. 5).

1. *Domain of cataclasites and shear zones*

In the northernmost outcrops, undeformed aplopegmatitic veins and granite dikes related to the late Hercynian SAN granite are intrusive into biotite micaschists. Slightly dipping north thrusts, outlined by cataclasites intimately associated with thin ultramylonite bands, sharply cut this assemblage. Some pegmatites have been boudinaged, and

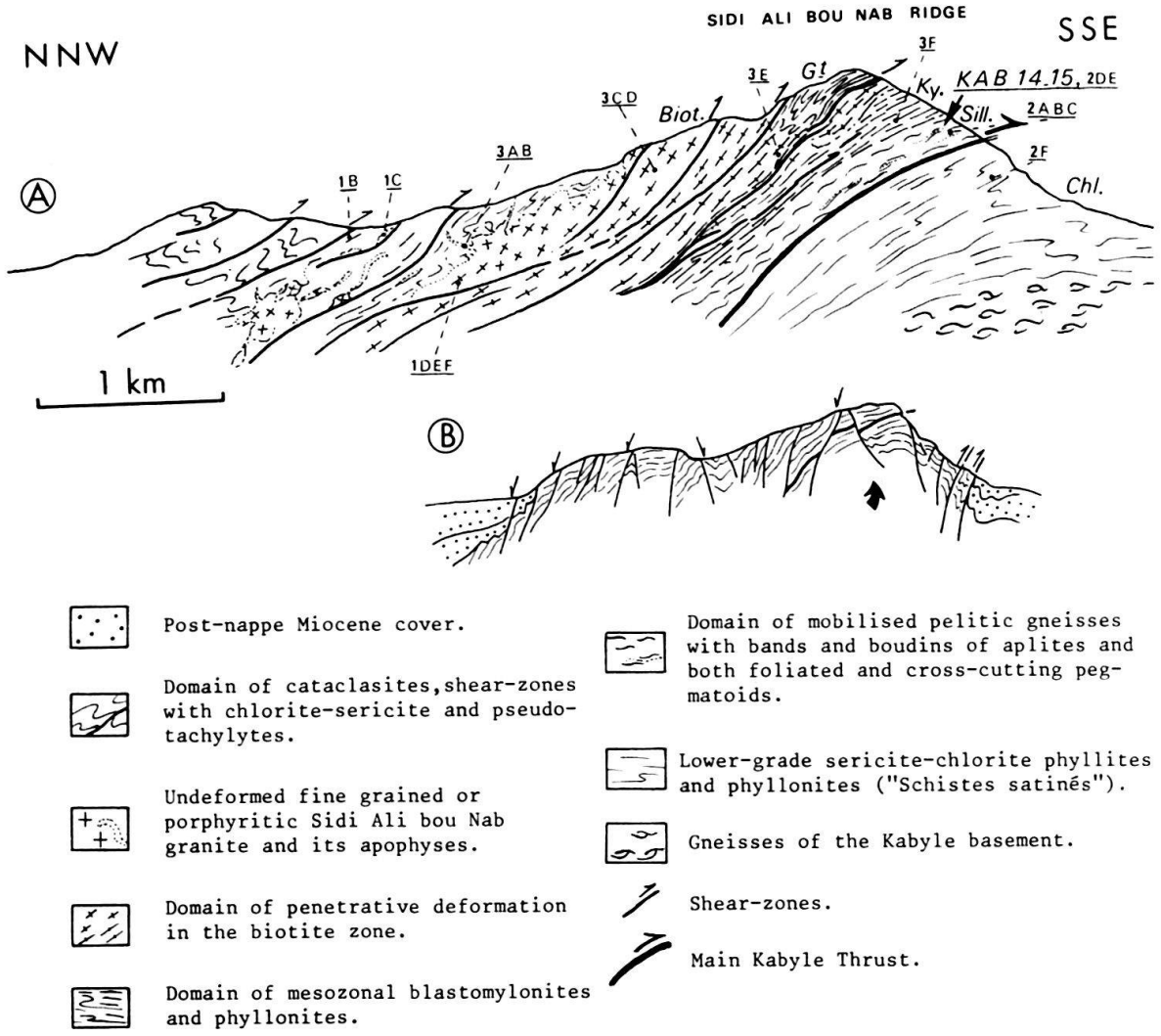

Fig. 5. A cross section through the Sidi Ali bou Nab blastomylonitic belt with samples and photographs location. A is an interpretative section which does not take into consideration the effects of post-Miocene uplift. B shows these effects of post-Miocene deformation. First appearances of biotite, garnet, kyanite and sillimanite are approximately indicated.

in thin section, quartz have a strong undulose extinction, with incipient mosaic recrystallization (Pl. 1, C). The ultramylonite bands exhibit a mosaic-porphyroclastic microstructure with a matrix in which small chlorite flakes represent the principal newly formed mineral.

Approaching some 350 m from the northern contact of the SAN granite subhorizontal shear zones increase in frequency. A planar structure progressively appears in plutonic rocks, grading into a mylonitic fabric within the shear zones. Phyllonite bands up to 1 m thick appear in micaschists. In these rocks, the new foliation is defined by chlorite and sericite with clasts of brown biotite and tourmaline (Pl. 1, B). When expressed, the stretching lineations and the slickensides outlined by chlorite, which are frequent on low angle fault planes, are mostly trending N–S. In the highly schistose rocks, chlorite crystallized in the pressure shadows of clasts demonstrating the low-temperature conditions and the pene-contemporaneous development of penetrative deformation in ultramylonites, phyllonitic rocks, and the low dipping faults with slickensides.

At the northern contact of the SAN granite, a very heterogeneous deformation can be observed. The pelitic hornfelses with unoriented andalusite still preserved are cut by veins and contorted apophyses of undeformed fine-grained or porphyritic granite, rich in pelitic xenoliths (Pl. 3, A).

These contact rocks possibly escaped penetrative deformation because of their rigid and unlayered nature. Some shear zones outlined by retrogressive minerals however transect these rocks, and entering some tens of meters into the granite body itself, a postmagmatic planar fabric rapidly appears in the muscovite-biotite granite. In thin section, a porphyroclastic fabric is outlined by strongly elongated quartz with undulose extinction and partial mosaic recrystallization.

Such contact rocks with brown biotite, garnet, andalusite, cordierite, K-feldspar, quartz and fresh fibrolite also surround the northern granite of Naciria. Textural relationships and the lack of any retrogressive mineral suggest equilibrium for this assemblage (Pl. 1, A).

The lack of deformation at the contact zone of a deformed granite has also been observed in the Hercynian granite du Pinet (Rouergue, Massif Central, France), the central part of which almost exhibits a postmagmatic mylonitic foliation, whereas the high-grade hornfelses and border apophyses escaped deformation (Burg & Teyssier 1983). Such a phenomenon has also been described in Carboniferous granites affected by Alpine events in the Zone du Grand Saint-Bernard (Caby 1968) and in the Grand Paradis orthogneisses (Bertrand 1968). Static pseudomorphs of Alpine kyanite after sillimanite have also been described in the later example by Compagnoni & Prato (1969).

2. *Domain of penetrative deformation in the biotite zone*

This domain progressively appears entering some hundreds of meters within the SAN granite body. A planar structure approximately E–W trending and dipping 20–40° north is developed everywhere (Pl. 3, B, C, D). In thin section, the cataclastic foliation is defined by newly formed synkinematic pale brown biotite. Optically and chemically different from the magmatic dark brown biotite, this secondary biotite has already been noticed by Bossière (1980). This secondary biotite is clearly synkinematic

since it is the principal mineral which has formed together with white mica in pressure shadows of quartz and feldspar clasts (Pl. 1, D). Some clasts of myrmekite are also conspicuous (Pl. 1, F). The matrix includes fine-grained quartz, acidic plagioclase and K-feldspar fragmented grains, and the mylonitic fabric of the rock is evident from plattenquartz with a secondary mosaic microstructure with well-pronounced preferred orientations (Pl. 1, E).

In several outcrops, we observed along the road the transition from a two-micas augengneiss into an ultramylonite over less than 1 m. In the ultramylonite, K-feldspar clasts are highly stretched with a pencil shape (shape ellipsoid in the range of 30/2.5/1).

Pendants and elongated xenoliths of pelitic rocks exhibit a mineral assemblage with biotite and white mica which can be ascertained as newly formed as demonstrated by undeformed biotite flakes in polygonal arcs which overgrew a secondary steep strain-slip cleavage.

3. *Domain of mesozonal blastomylonites and phyllonites*

These rocks are well-exposed all along the SAN ridge and have been already described by BOSSIÈRE & VAUCHEZ (1978) and BOSSIÈRE (1980). This domain may be traced at the root of the SAN granite, and a gradual transition with the previous domain can be inferred.

The rocks of this domain are mostly fine-grained phyllonitic schists interbanded with leucocratic mylonites (Pl. 3, E) which have been proved on chemical grounds to derive from aplite and granite dikes (BOSSIÈRE 1980).

Mineral associations of pelitic rocks include biotite + white mica + almandine ± staurolite ± kyanite; those from leucocratic mylonites include acidic plagioclase + microcline + garnet ± kyanite with a mosaic microstructure.

In the pelitic rocks, both syn- and postkinematic growths of micas and Al-silicates, and the lack of any noticeable retrograde alterations indicate that we are dealing with blastomylonites s.s. of amphibolite facies grade (BOSSIÈRE 1980).

Structure of blastomylonites. The mylonitic banding mainly exhibits a 20°–45°N northward dip. A linear fabric is conspicuous, gently dipping NNW–NW. This linear fabric has formed in a early stage of deformation with mylonitic banding, which has been later involved in complex folding. The various trend of metric scale isoclinal fold would indicate a highly ductile behaviour of these blastomylonites, and such a complex, often disharmonic folding has been frequently reported in several ultramylonites. Curviplanar folds, eye-shaped sections of folds, and nose-type closures are conspicuous of sheath folds which have been observed on a small scale only (Fig. 6). Folding of the linear fabric in the nose of these structures are in agreement with tectonic transport towards ESE–SE, though no systematic measurements have been done.

4. *Domain of mobilized pelitic gneisses*

The mesozonal phyllonites described above seem to pass gradually downwards into higher grade pelitic gneisses of similar composition, with bands and boudins of leucocratic, fine-grained metaaplites (Pl. 3, F). These pelitic gneisses differ from those described above by a coarser grained mineral association with biotite + muscovite + K-

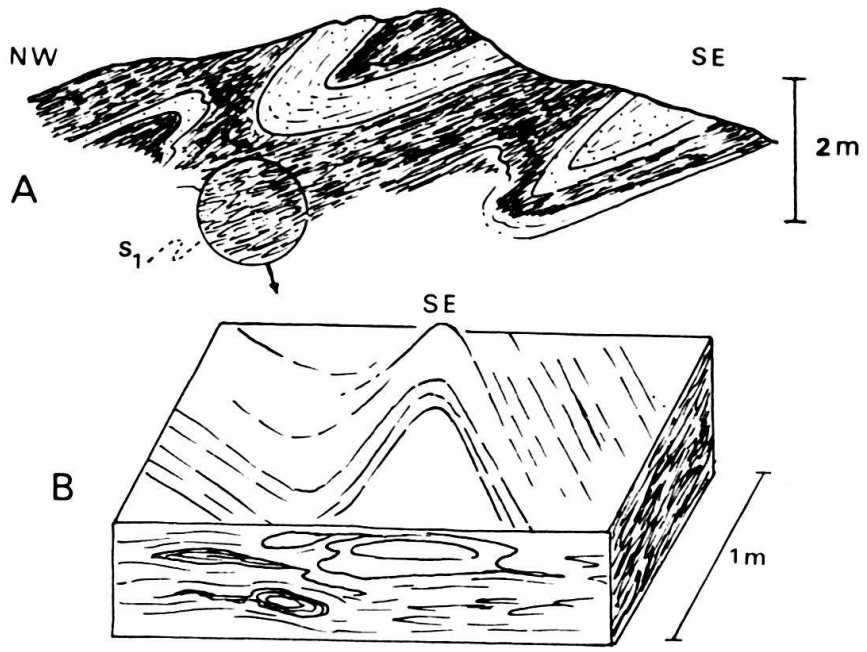

Fig. 6. Phyllonitic micaschists along the Sidi Ali bou Nab ridge. The mylonitic foliation well expressed by quartz ribbons in leucocratic ultramylonites (dotted) is folded by "second phase" recumbent folds with E–W axes (A). Stretching lineations in those rocks trend similarly to N-130 in both limbs of folds. In the phyllonitic micaschists (in grey), the blastesis of fresh biotite and muscovite (already present within the mylonitic S_1 plane) and garnet, staurolite ± kyanite is also syn to late kinematic in respect to the post foliation "second phase" folds. Within the S_2 plane (B), stretching lineations are curved and define curviplanar to festoon folds facing southeast with eye shaped sections (drawn after photographs).

feldspar + kyanite + garnet + graphite together with fine-grained micas and sillimanite in the matrix and pressure shadows, and polycrystalline plattenquartz (Pl. 2, A, B, C). The Al-silicates and feldspar most frequently have the shape of asymmetric augen or "cornues", but they also constitute streaks and films whereas the coarser-grained micas generally exhibit a sigmoidal shape.

Intrafolial leucosomes varying in thickness from about 10 cm to some meters with a gneissic fabric appear to be less deformed than their country rocks. The primary mineralogy contains microcline, acidic plagioclase, quartz, muscovite, garnet and tourmaline ± biotite (Pl. 2, D). Associated with the blastomylonitic foliation, synkinematic parageneses with fine muscovite + garnet + kyanite + sillimanite ± biotite partly obliterate the primary assemblage (Pl. 2, E). No sign of any retrogression in these rocks is noticeable. Some cross-cutting leucosome pegmatoids have also been observed.

For ^{39}Ar–^{40}Ar dating, we have selected two samples in this domain where the blastomylonitic event reached its highest grade. Sample KAB 14 is a completely recrystallized intrafolial metaaplite which foliation plane is underlined by recrystallized and newly formed white mica and late biotite, with only some relicts of primary plagioclase and tourmaline. Sample KAB 15 is a foliated coarse-grained metapegmatite with eye-shaped clasts of K-feldspar and muscovite preserved in a matrix in which tinny secondary flakes of muscovite define the foliation (Pl. 3, E). Owing to their different natural grain size, the two muscovite generations have been separated for dating.

5. *The zone of sericite–chlorite phyllites and phyllonites*

This much lower grade unit outcrops below the pelitic gneisses, and generally exhibits a subhorizontal cleavage. A major metamorphic and structural discontinuity necessarily occurs between both units, and this discontinuity is clearly expressed in the morphology, with a narrow plateau on the steep southern flank of the mountain. The collected rocks are chlorite–white-mica rich phyllites (Pl. 2, F) which belong to the "Série satinée" of BOSSIÈRE (1980). Oxychlorite and possible pale brown biotite are also present, with small garnets in equilibrium(?) with albite. Some aplite bands with a random microstructure are also present.

Discussion

According to these petrographic and structural data, the SAN granite obviously predates the thermotectonic event during which the blastomylonites were generated. Two main events have been identified within the SAN blastomylonitic belt.

1. The attitude of linear fabrics in blastomylonites and the trend of sheath folds would indicate a foremost synmetamorphic movement toward the ESE to SE. In the visited area, the prograde mylonitic deformation may be considered as the result of a major oblique thrusting of the northern higher grade rocks with a normal vertical gradient (i.e. a north-dipping dextral wrench fault).
2. Below the blastomylonites, the occurrence of a strong metamorphic inversion implies a young southward thrusting of the metamorphic rocks and blastomylonites with a cold tectonic contact. As a consequence, the higher grade gneisses suffered a low temperature retromorphic process restricted to some tens of meters along the thrust plane.

Thus, the observations performed along the N–S section of the SAN ridge show the characteristics of a major postmetamorphic shear zone, in many regards similar to many other deep thrust zones of the Himalaya type (M.C.T., PÊCHER 1978; CABY et al. 1983, French Massif Central, BURG & MATTE 1978, PIN 1979).

In Petite-Kabylie, the Beni Ferguen blastomylonitic belt has been shown to reflect analogous metamorphic and structural relationships (BOUILLIN 1982a, b) and it is suggested that these two fundamental lineaments within the Kabyle basement are related to the same tectonometamorphic episode. However, the overall stratigraphic, structural and metamorphic markers do not yet allow to decide whether the blastomylonitic event was Hercynian (BOSSIÈRE 1980) or Alpine in age. Within the SAN area, Rb–Sr biotite ages lead to the recognition of Alpine events (PEUCAT & BOSSIÈRE 1981) but their significance with respect to the metamorphic evolution remained debatable. These Alpine ages were interpreted by their authors as only a reflect of a thermal episode confined within a Hercynian blastomylonitic belt which would have behaved as a guide of heat flow during Alpine orogeny.

Our view is quite different. The mylonitic deformation may be considered as a prograde metamorphism which affected a Hercynian granite and its country rocks; the tectonometamorphic characters of the SAN cross section have demonstrated clearly that shearing was occurring after granite emplacement and as pointed out by BOSSIÈRE (1980) after the regional metamorphic overprint.

Age of the blastomylonitic deformation of Sidi Ali bou Nab

The ^{39}Ar–^{40}Ar stepwise heating method has been applied to pure mineral fractions of biotite and muscovite from the fine-grained KAB 14 and coarse-grained KAB 15 leucosomes. On the basis of granulometric criteria, we have made a distinction between the prekinematic and synkinematic muscovites from this latter sample. Microprobe analyses of BOSSIÈRE (1980, 1983) and our data indicate that the primary white mica is represented by a pure muscovite whilst the latter shows a slightly higher celadonite content ($\leq Si_{3.1}$).

Muscovite concentrate separated from sample KAB 14 gives a flat apparent age spectrum defining a plateau for more than 99% of all the gas released (Fig. 7, a). The total gas age and plateau age are concordant at 25.6 ± 0.7 m.y. and 25.7 ± 0.7 m.y. respectively. The age spectrum for the coexisting metamorphic biotite (Fig. 7, b) exhibits more internal discordance; however, approximately 85% of all the gas released records a plateau age of 24.7 ± 1.3 m.y., consistent within the 2 σ analytic errors limits with the plateau age determined on muscovite. Initial low-temperature increments reflect younger ages with a minimum value at 12.5 ± 3.3 m.y. which may be related to a late disturbance.

The apparent ^{39}Ar–^{40}Ar ages recorded by the syntectonic muscovite from the coarse-grained pegmatite (KAB 15.2) define an age spectrum displaying a plateau at 24.9 ± 0.6 m.y. related to more than 99% of the ^{39}Ar released (Fig. 8, a). The total gas age is 24.8 ± 0.6 m.y. This age is in good agreement with the above data on coexisting syntectonic biotite and muscovite KAB 14 and also with Rb–Sr ages (22–38 m.y.) on biotites from the SAN granite (PEUCAT & BOSSIÈRE 1981). For each sample, plotting the data in a $^{40}Ar/^{36}Ar$ vs $^{39}Ar/^{36}Ar$ correlation diagram yields a well-defined isochron age concordant with the plateau age and a trapped argon composition defined by the ordinate intercept close to the atmospheric composition (Table 2).

In addition, ^{39}Ar–^{40}Ar investigations have been carried out on a single porphyroblast of primary muscovite from sample KAB 15 (Pl. 2, E) in order to provide some information on the age of the pegmatite segregation process.

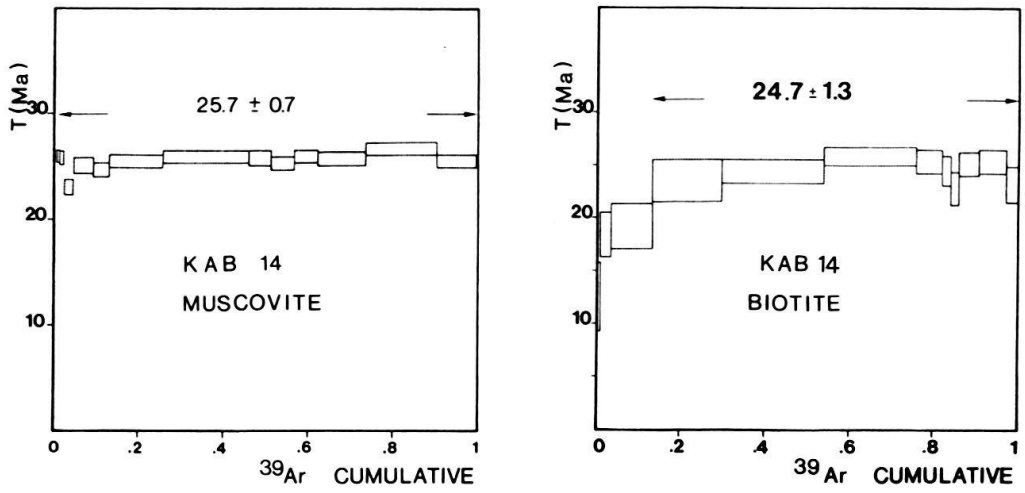

Fig. 7. Apparent age spectra of syntectonic muscovite (a) and biotite (b) from the blastomylonitic fine-grained pegmatites of Sidi Ali bou Nab.

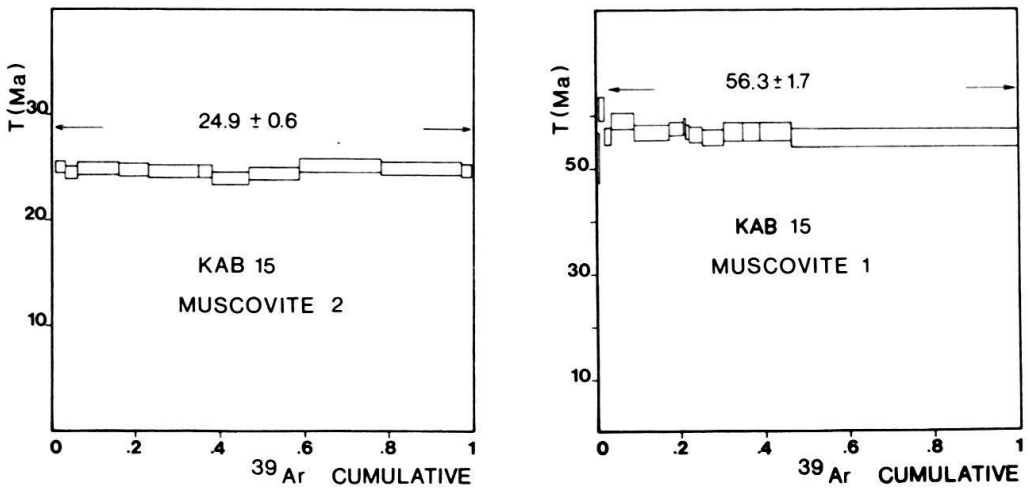

Fig. 8. Apparent age spectra of syntectonic muscovite KAB 15.2 (a) and prekinematic muscovite KAB 15.1 (b) from the blastomylonitic coarse-grained pegmatites of Sidi Ali bou Nab.

An artificial granulometric fraction of 80–100 μm was obtained from this crystal by careful hand crushing and sieving. The apparent age spectrum (Fig. 8, b) displays a well-defined plateau age of 56.3 ± 1.7 m.y. for 98% of the ^{39}Ar released (total age at 56.4 ± 1.7 m.y.). This age pattern may receive different interpretations:

— First, we may consider that this age spectrum is characteristic of an undisturbed system formed 56 m.y. ago, and which has survived without loss of radiogenic argon the subsequent blastomylonitic event at 25 m.y.
— Alternatively, we may interpret the 56 m.y. age as an age intermediate between two events, thus without geological significance. However there is evidence that thermally and/or tectonically overprinted muscovites usually display age spectra similar to those predicted by TURNER's (1968) volume diffusion model, with a progressive increase in age from the low-temperature steps (HANSON et al. 1975; ALBARÈDE et al. 1978; HARRISON & MC DOUGALL 1981; MONIÉ & MALUSKI 1983). Such an age pattern has been observed for the Algiers muscovite AG 1.
— Finally, we may assume that the 56 m.y. plateau is an anomalously old age due to uniform incorporation of excess radiogenic argon in muscovite. However, such a uniform gain of ^{40}Ar in muscovite has, to our knowledge, never been reported whereas biotites containing proved excess argon are well-documented (see the review by FOLAND 1983). Moreover, plotting our ^{39}Ar–^{40}Ar data in $^{40}Ar/^{36}Ar$ vs $^{39}Ar/^{36}Ar$ and $^{39}Ar/^{40}Ar$ vs $^{36}Ar/^{40}Ar$ isotope correlation diagrams yields no evidence of argon gain or loss.

In their Rb–Sr study, PEUCAT & BOSSIÈRE (1981) reported whole-rock and mineral dates which suggest a late Hercynian age (ca. 260 m.y. whole-rock isochron) for the undeformed pegmatites collected within the southern Kabyle basement and near Tizi Ouzou. Assuming the coarse-grained leucosome KAB 15 to belong to the same Hercynian pegmatitic segregates, the 56 m.y. plateau age would be a false plateau related to a uniform loss of radiogenic argon during the 25 m.y. event. In this case, this age spectrum is effectively indistinguishable from the spectra of undisturbed samples. None

of the apparent ages gives unequivocally evidence for this homogeneous partial resetting of the coarse muscovite.

However, such an argon behaviour appears to be in conflict with the TURNER'S model (1968). In our view, this unusual pattern of argon liberation from sample KAB 15-1, and mainly the resistance of the less retentive sites to complete rejuvenation, may be due to the large natural grain size and undeformed character of the muscovite.

Estimated conditions for the blastomylonitic event are $P > 6$ Kb, $T = 640 \pm 50$ °C (BOSSIÈRE 1980). The lack of anatectic melting and considerations on the phase compatibilities suggest that low PH_2O conditions have prevailed during the early Miocene event. Under such limited fluid mobility conditions, it is possible that undeformed coarse-grained muscovite has partially preserved its initial fluids content despite temperatures above 600 °C. Thus, if the evaluation of the P and T parameters is reliable, the behaviour of the argon is noticeable due to the lack of total resetting.

A possible further evidence of the resistance of the primary KAB 15 muscovite to complete argon loss may be provided from the isotopic data by evaluating the nonradiogenic trapped argon. $^{40}Ar/^{39}Ar$ vs $^{39}Ar/^{36}Ar$ isochron diagrams indicate for both muscovite generations an atmospheric composition for this trapped argon. However, the data show an important difference in ^{36}Ar concentration between these generations. Secondary muscovite yields an ^{36}Ar concentration of 1.266×10^{-13} moles/g while an ^{36}Ar concentration ten times greater of 1.011×10^{-12} moles/g is obtained for the primary muscovite. As this atmospheric component is mainly released in the high-temperature fractions (> 800 °C), it is suggested that it has been trapped within the coarse muscovite during its crystallization and not incorporated during a subsequent disturbance. Thus, it appears that the primary muscovite was formed under a relatively high argon pressure of atmospheric composition, which is consistent with the fluid pressure conditions which usually prevail during a pegmatite segregation process. This great proportion of trapped ^{36}Ar correlated with radiogenic ^{40}Ar indicates that the coarse-grained muscovite has not exchanged all of its argon content during the subsequent high-grade metamorphism at 25 m.y.

It is suggested that deformation and recrystallization have promoted an atmospheric and radiogenic argon reequilibration of the finer-grained muscovites to the conditions of the overprinting metamorphism as newly formed muscovites appear mainly by the breakdown of K-feldspar.

Conclusions and consequences

In the light of the above mentioned constraints provided by an associated tectonometamorphic study together with independent ^{39}Ar–^{40}Ar geochronological controls, a new interpretation of the geological evolution within the inner zones of Grande-Kabylie is proposed.

The eo-Alpine age (85–95 m.y.) suggested for the high temperature regional metamorphism is quite different than the Pan-African age currently accorded to this event. A number of isotopic data, previously interpreted to represent a thermal event without metamorphic imprint, is consistent with the proposed new age. Moreover, this age is in agreement with the age of the major tectonometamorphic events recorded within the southern external domain. This result implies that the sedimentary pile comprising a

stratigraphic sequence of late Cambrian and traditionally thought to be the autochthonous to para-autochthonous cover of the Kabyle basement represents an allochthonous unit thrusted upon this crystalline basement during the Alpine orogeny.

Obviously, the lack of Hercynian or older ^{39}Ar–^{40}Ar ages is not conflicting with the existence of Hercynian or Pan-African metamorphic and plutonic events as previously recorded by PEUCAT & BOSSIÈRE (1980).

In Grande-Kabylie, a major recrystallization episode restricted to the Djebel Sidi Ali bou Nab area took place under chlorite to sillimanite metamorphic conditions at the expense of metamorphic and plutonic assemblages of Hercynian age. From a N–S section across the SAN blastomylonitic belt, a regular distribution pattern of metamorphic parageneses and structures with a systematic increase of metamorphic grade from the north to the south has been recognized. This regular pattern is related to the motion of the SAN shear zone as a north dipping dextral wrench fault, bringing the northern higher grade rocks upon lower grade phyllites of the Kabyle basement.

Three syntectonic micas dated by the step-degassing ^{39}Ar–^{40}Ar method give concordant age data which point out to a late Oligocene–early Miocene age for this blastomylonitic event. The biotite KAB 14 is interpreted to have been partially reset during the late phase of southeastward overthrusting, locally bringing the northern part of the Kabyle basement upon the post-nappe Miocene cover.

The present ^{39}Ar–^{40}Ar results also indicate that under some circumstances it is possible to find in the same rock micas which remained isotopically closed since their formation and micas which have been totally reset during a subsequent metamorphic event, coexisting with a newly formed generation.

As the estimated thermal conditions for the SAN recrystallization episode exceed by far the usually assumed closure temperature for argon diffusion in muscovite, it is suggested that temperature is not the prevailing parameter which promotes argon loss. Our radiometric data require that recrystallization and penetrative deformation, which are known to be temperature-dependent processes, have induced the observed isotopic readjustments, coupled with chemical changes, of the finer muscovite. In this respect, we may assume that the temperature of complete opening of the coarse-grained undeformed muscovite is not the same as its closure temperature during the cooling of the pegmatite. As suggested by CHOPIN & MALUSKI (1980, 1982) and DODSON (1981), the "blocking temperature concept" should be carefully used, mainly when one address to complex geological areas, as it tends to superpose two different argon diffusion properties. These observations agree with recent contributions (VERSCHURE et al. 1980; DEUTSCH & STEIGER 1983) which have shown that two coexisting mineral generations of the same species could yield two sets of geologically meaningful ages.

REFERENCES

ALBARÈDE, F., FÉRAUD, G., KANEOKA, I., & ALLÈGRE, C.J. (1978): ^{39}Ar–^{40}Ar dating: the importance of K-feldspars on multi-mineral data of polyorogenic areas. – J. Geol. *86*, 581–598.

ALEXANDER, E.C., MICKELSON, G.M., & LANPHERE, M.A. (1978): MMHb.1: A new $^{40}Ar/^{39}Ar$ dating standard. – Short pap. 4th Int. Conf. Geochron. Cosmochron. Isot. geol. US, p.6–8.

BAUDELOT, S., & GÉRY, B. (1979): Découverte d'Acritarches du Cambrien supérieur et du Trémadoc dans le massif ancien de Grande-Kabylie. – C.R. Acad. Sci. (Paris) *288*, 1513–1516.

BELLON, H. (1976): Séries magmatiques Néogènes et quaternaires du pourtour de la Mediterranée occidentale, comparées dans leur cadre géochronométrique; implications géodynamiques. – Thèse Doctorat Orsay.

BERGER, C.W. (1975): $^{40}Ar/^{39}Ar$ step heating of thermally overprinted biotite hornblende and potassium feldspar from Eldora, Colorado. – Earth and planet. Sci. Lett. *26*, 375–408.

BERTRAND, J.M. (1968): Etude structurale du versant occidental du massif du Grand-Paradis (Alpes Graies). – Géol. alp. *44*, 55–87.

BLANC, P., & OBERT, D. (1974): Le métamorphisme lié à la phase tectonique anté-cénomanienne du domaine tellien septentrional (Babors, Algérie). – Bull. Soc. géol. France (7), *21*, 189–193.

BLÈS, J.L. (1971): Etude tectonique et microtectonique d'un massif autochtone tellien et sa couverture de nappes: le massif de Blida (Algérie du Nord). – Bull. Soc. géol. France (7), *13*, 498–511.

BOSSIÈRE, G. (1975): Une phase tectonique de haute pression en Grande-Kabylie (Algérie): les blastomylonites de Sidi Ali bou Nab. – 3e Réun. ann. Sci. Terre Montpellier, p. 59.

— (1977): Sur l'existence d'une bande blastomylonitique au Nord-Ouest de la Grande-Kabylie. – Bull. Soc. géol. France (7), *19*, 1071–1076.

— (1980): Un complexe métamorphique polycyclique et sa blastomylonitisation. Etude pétrologique de la partie occidentale du massif de Grande-Kabylie (Algérie). – Thèse Doctorat Nantes.

— (1983): Variations in muscovite and feldspar compositions during mylonitisation. – Abstr. 2nd E.U.G. Meet. Strasbourg. Terra Cognita *3*, p. 245.

BOSSIÈRE, G., & VAUCHEZ, A. (1978): Déformation naturelle par cisaillement ductile d'un granite de Grande-Kabylie occidentale (Algérie). – Tectonophysics *51*, 57–81.

BOUILLIN, J.P. (1977): Géologie de la Petite-Kabylie dans les régions de Collo et d'El Milia (Algérie). – Trav. Lab. Géol. méditerr. Assoc. CNRS, Paris.

— (1982a): Mise en évidence d'un important accident blastomylonitique dans le Nord de la Petite-Kabylie (Algérie). – C.R. Acad. Sci. Paris *294*, 1233–1236.

— (1982b): Mise en évidence d'importantes structures tangentielles au sein du socle de Petite-Kabylie (Algérie). – C.R. Acad. Sci. Paris *294*, 1271–1274.

BOUILLIN, J.P., & KORNPROBST, J. (1974): Associations ultrabasiques de Petite-Kabylie: péridotites de type alpin et complexe stratifié; comparaison avec les zones internes bético-rifaines. – Bull. Soc. géol. France (7), *16*, 183–194.

BRERETON, N.R. (1970): Corrections for interfering isotopes in the $^{40}Ar/^{39}Ar$ dating method. – Earth and planet. Sci. Lett. *8*, 427–433.

BURG, J.P., & MATTE, P. (1978): A cross section through the French Massif Central and the Scope of its Variscan Geodynamic Evolution. – Z.dtsch.geol.Ges. *129*, 429–460.

BURG, J.P., & TEYSSIER, C. (1983): Contribution à l'étude tectonique et microtectonique des séries cristallophylliennes du Rouergue oriental. La déformation des laccolites syntectoniques, type Pinet. – Bull. Bur. Rech. géol. min. (2), *1*, sér. Géol. France, 2e sér., 3–30.

CABY, R. (1968): Contribution à l'étude structurale des Alpes occidentales. Subdivisions stratigraphiques et structure de la zone du Grand Saint-Bernard dans la partie Sud du Val d'Aoste (Italie). – Trav. Lab. Géol. Fac. Sci. Grenoble *44*, 95–111.

— (1982): Données nouvelles sur la tectonique tangentielle en Grande-Kabylie: existence d'un chevauchement majeur alpin de type himalayen. – 9e Réun. ann. Sci. Terre Paris, p. 105.

CABY, R., PÊCHER, A., & LE FORT, P. (1983): Le grand chevauchement central himalayen: nouvelles données sur le métamorphisme inverse à la base de la Dalle du Tibet. – Rev. Géol. dyn. Géogr. phys. *24*, 89–100.

CAIRE, A. (1975): Essai de coordination des accidents transversaux en Algérie et en Tunisie. – C.R. Acad. Sci. Paris *280*, 403–406.

CHOPIN, C., & MALUSKI, H. (1980): $^{40}Ar/^{39}Ar$ dating of high-pressure metamorphic micas from the Gran Paradiso area (Western Alps): evidence against the blocking temperature concept. – Contr. Mineral. Petrol. *74*, 109–122.

— (1982): Unconvincing evidence against the blocking temperature concept. A reply. – Contr. Mineral. Petrol. *80*, 391–394.

COMPAGNONI, R., & PRATO, R. (1969): Paramorfosi di cianite su sillimanite in scisti pregranitici nel massicio del Gran Paradiso. – Boll. Soc. geol. ital. *88*, 537–549.

DALLMEYER, R.D. (1982): $^{40}Ar/^{39}Ar$ incremental release of biotite from a progressively remetamorphosed Archean basement terrane in Southwestern Labrador. – Earth and planet. Sci. Lett. *61*, 85–96.

DEUTSCH, A., & STEIGER, R.H. (1983): Formation ages vs. cooling ages: K–Ar dating on amphiboles from the Central Alps. – Abstr. 2nd E.U.G. Meet. Strasbourg. Terra Cognita *3*, p. 138.

DEVAUX, J. (1969): Recherche de l'organisation des contraintes dans le tréfonds de l'Algérie du Nord. Rôle des failles de décrochement obliques sur l'Ouest. – Bull. Serv. Carte géol. Algérie [n.s.] *39*, 41–69.

DODSON, M.H. (1981): Thermochronometry. – Nature *293*, 606–607.

DURAND-DELGA, M. (1951): L'âge du métamorphisme général du massif de Petite-Kabylie. – C.R. Acad. Sci. Paris *232*, 745–747.

— (1955): Etude géologique de l'Ouest de la chaîne numidique. – Thèse Paris.

— (1969): Mise au point sur la structure du Nord-Est de la Berbérie. – Bull. Serv. Carte géol. Algérie *39*, 89–131.

FOLAND, K.A. (1983): $^{40}Ar/^{39}Ar$ incremental heating plateaus for biotites with excess argon. – Isotope Geosci. *41*/1, 3–21.

FREY, M., HUNZIKER, J.C., O'NEIL, J., & SCHWANDER, H.W. (1976): Equilibrium disequilibrium relations in the Monte-Rosa granite, Western Alps: Petrological, Rb–Sr and stable isotope data. – Contr. Mineral. Petrol. *55*, 147–179.

GÉLARD, J.P. (1979): Géologie du Nord-Est de la Grande-Kabylie. – Mém. géol. Univ. Dijon *5*.

HANSON, G.N., SIMMONS, K.R., & BENCE, A.E. (1975): $^{40}Ar/^{39}Ar$ spectrum ages for biotite hornblende and muscovite in a contact metamorphic zone. – Geochim. cosmochim. Acta *39*, 1269–1277.

HARRISON, T.M., & MC DOUGALL, I. (1980): Investigations of an intrusive contact, Northwest Nelson, New Zealand, II. Diffusion of radiogenic and excess ^{40}Ar in hornblende revealed by $^{40}Ar/^{39}Ar$ age spectrum analyses. – Geochim. cosmochim. Acta *44*, 2005–2020.

— (1981): Excess ^{40}Ar in metamorphic rocks from Broken Hill, New South Wales: implications for $^{40}Ar/^{39}Ar$ age spectra and the thermal history of the region. – Earth and planet. Sci. Lett. *55*, 123–149.

LEPVRIER, C. (1971): Données relatives à la schistosité et au métamorphisme dans les massifs du Chélif et du Bou Maad (autochtone Nord et mésotellien, Algérie). – C.R. Acad. Sci. Paris *273*, 284–286.

LOOMIS, T.P. (1975): Tertiary mantle diapirism, orogeny, and plate tectonics East of the Strait of Gibraltar. – Amer. J. Sci. *275*, 1–30.

MAHDJOUB, Y. (1981): La déformation plastique d'échelle microscopique dans les unités tectoniques du massif d'Alger. Un écaillage contemporain de la mylonitisation épizonale. – Thèse 3e cycle Alger.

— (1982): Un cisaillement ductile vers l'Est: stage précoce de la mylonitisation du massif d'Alger. – 9e Réun. ann. Sci. Terre Paris, p. 396.

MALUSKI, H. (1978): Behaviour of biotites, amphiboles, plagioclases and K-feldspars in response to tectonic events with the $^{40}Ar/^{39}Ar$ radiometric method. Example of Corsican granite. – Geochim. cosmochim. Acta *42*, 1619–1633.

MALUSKI, H., LEPVRIER, C., & BIARDEAU, V. (1979): Epimétamorphisme syntectonique d'âge 80 MA dans les zones Nord-telliennes (Algérie). – C.R. Acad. Sci. Paris *288*, 1583–1586.

MATTAUER, M. (1963): Le style tectonique des chaînes telliennes et rifaines. – Geol. Rdsch. *53*, 296–313.

MICHARD, A., CHALOUAN, A., MONTIGNY, R., & OUAZZANI-TOUHAMI, M. (1983): Les nappes cristallophylliennes du Rif (Sebtides, Maroc), témoins d'un édifice alpin de type pennique incluant le manteau supérieur. – C.R. Acad. Sci. Paris *296*, 1337–1340.

MONIÉ, P., & MALUSKI, H. (1983): Données géochronologiques $^{40}Ar/^{39}Ar$ sur le socle anté-Permien du massif de l'Argentera–Mercantour (Alpes Maritimes, France). – Bull. Soc. géol. France (7), *25*, 247–257.

MONIÉ, P., MALUSKI, H., CABY, R., & SAADALLAH, A. (1982): Age à 85 Ma par la méthode ^{39}Ar–^{40}Ar du métamorphisme de haute température du massif d'Alger. – C.R. Acad. Sci. Paris *295*, 935–938.

OBERT, D. (1974): Phases tectoniques d'âge anté-cénomanien dans les Babors (Tell Nord-sétifien, Algérie). – Bull. Soc. géol. France (7), *16*, 171–176.

PÊCHER, A. (1978): Déformation et métamorphisme associé à une zone de cisaillement. Exemple du Grand Chevauchement Central Himalayen (MCT), transversale des Annapurnas et du Manaslu, Népal. – Thèse Doctorat Grenoble.

PEUCAT, J.J., & BOSSIÈRE, G. (1978): Mise en évidence d'un plutonisme paléozoïque inférieur en Grande-Kabylie (Algérie). – 6e Réun. ann. Sci. Terre Orsay, p. 108.

— (1981): Ages Rb–Sr sur micas du socle métamorphique Kabyle (Algérie): mise en évidence d'événements thermiques alpins. – Bull. Soc. géol. France (7), *23*, 439–447.

PIN, C. (1979): Géochronologie U–Pb et microtectonique des séries métamorphiques anté-Stéphaniennes de l'Aubrac et de la région de Marvejols (Massif Central). – Thèse 3e cycle Montpellier.

POLVÉ, M., & ALLÈGRE, C.J. (1982): The upper mantle-lower crust transition studied with Rb–Sr, Sm–Nd systematics. Examples from Beni Bousera and Lanzo. – Abstr. 5th Conf. Geochron. Cosmochron. Isot. geol. Japan, p. 312.

PUGA, E. (1977): Sur l'existence dans le complexe de la Sierra Nevada (Cordillère Bétique, Espagne du Sud) d'éclogites et sur leur origine probable à partir d'une croûte océanique Mésozoïque. – C. R. Acad. Sci. Paris *285*, 1379–1382.

RAOULT, J.F. (1974): Géologie du Centre de la chaîne numidique (Nord du Constantinois, Algérie). – Mém. Soc. géol. France *53*/121.

SAADALLAH, A. (1981): Le massif cristallophyllien d'El Djazair (Algérie). Evolution d'un charriage à vergence Nord dans les Internides des Maghrébides. – Thèse 3e cycle Alger.

— (1982): Ecailles de socle dans le massif d'Alger: exemple d'un processus continu de déformation, lors d'un charriage d'âge alpin(?) à vergence Nord. – 9e Réun. ann. Sci. Terre Paris, p. 561.

STEIGER, R.H., & JÄGER, E. (1977): Subcommission on Geochronology: convention on the use of decay constants in geo- and cosmochronology. – Earth and planet. Sci. Lett. *36*, 359–362.

TORRES-ROLDÁN, R. (1979): The tectonic subdivision of the Betic Zone (Betic Cordilleras, Southern Spain). Its significance and one possible geotectonic scenario for the Westernmost Alpine belt. – Amer. J. Sci. *279*, 19–51.

TURNER, G. (1968): The distribution of potassium and argon in chondrites. In: AHRENDS, L.H. (Ed.): Origin and Distribution of the Elements (p. 387–398). – Pergamon, Oxford.

VERSCHURE, R.H., ANDRESSEN, P.A.M., BOELRIJK, N.A.I.M., HEBEDA, E.H., MAIJER, C., PRIEM, H.N.A., & VERDURMEN, E.A.T. (1980): On the thermal stability of Rb–Sr and K–Ar biotite systems: evidence from coexisting Sveconorwegian (ca 870MA) and Caledonian (ca 400MA) biotites in SW Norway. – Contr. Mineral. Petrol. *74*, 245–252.

VILA, J.M. (1980): La chaîne alpine d'Algérie Orientale et des confins Algéro-Tunisiens. – Thèse Doctorat Paris.

WILDI, W. (1983): La chaîne tello-rifaine (Algérie, Maroc, Tunisie): structure, stratigraphie et évolution du Trias au Miocène. – Rev. Géol. dyn. Géogr. phys. *24*, 201–297.

YORK, D. (1969): Least square fitting of a straight line with correlated errors. – Earth and planet. Sci. Lett. *5*, 320–324.

Plate 1

Fig. A — High grade hornfels from the Naciria inlier, with fresh garnet porphyroblasts and biotite (A_1) and fresh fibrolite at grain boundaries (A_2). × 60.

Fig. B — Low grade phyllonitic schist. The mylonitic foliation is defined by tinny chlorite and white micas, with dispersed clasts of quartz, biotite and tourmaline. × 40.

Fig. C — Mylonitic pegmatite with a mosaic-porphyroclastic microstructure. Note the truncated K-feldspar clasts and the incipient recrystallization of quartz grains with a mosaic habitus, indicating low temperature. × 60.

Fig. D — Foliated porphyritic granite, with augen of K-feldspar; newly formed brown microbiotite is present in the matrix. × 60.

Fig. E — Mylonitic orthogneiss exhibiting ribbon of quartz and sygmoidal clasts of K-feldspar. × 60.

Fig. F — Orthogneiss with a clast of myrmekitic K-feldspar in a completely recrystallized matrix with secondary microcline and biotite. × 60.

A_1

A_2

B

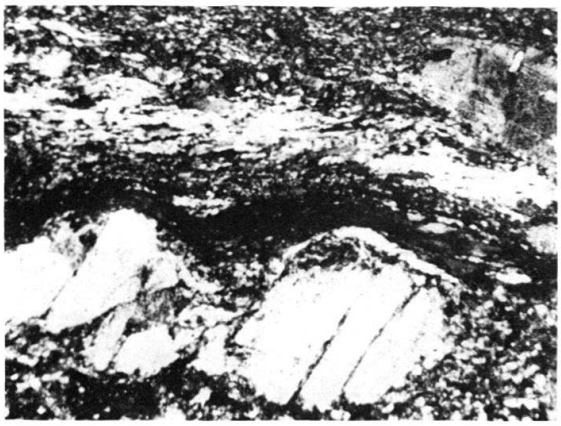

C

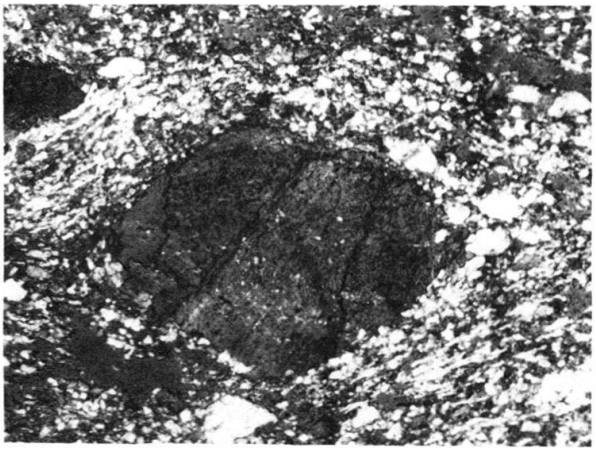

D

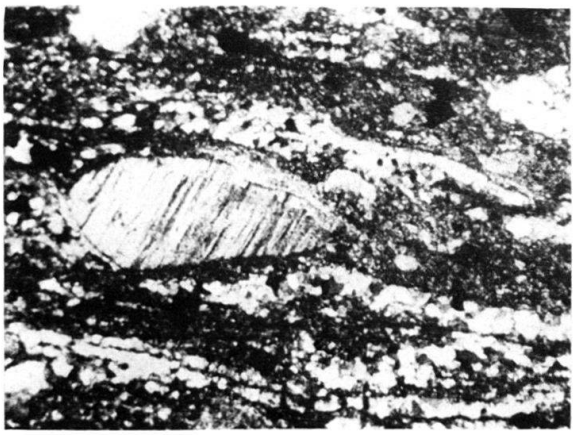

E

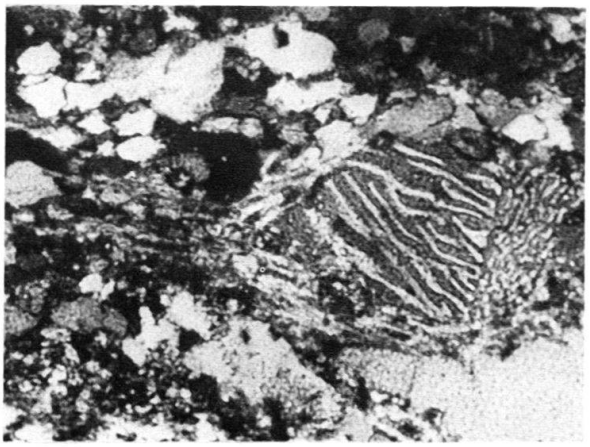

F

Plate 2

Fig. A Mylonitic micaschist. Note the laminated ribbon of quartz and the augen of Al silicates surrounded by films of brown red biotite. × 40.

Fig. B Idem. Eye-shaped porphyroblast of garnet enveloped by red biotite. × 40.

Fig. C Polycrystalline porphyroblast of kyanite. Fresh fibrolite is also present in the biotite envelop and in quartz. × 60.

Fig. D Mylonitic pegmatite cutting kyanite micaschists. Microcline augen are separated by ribbons of quartz. × 20.

Fig. E Idem. Large muscovite porphyroclasts with secondary white mica recrystallized in pressure shadows. × 20. Sample KAB 15.

Fig. F Phyllite with the development of a strain-slip horizontal schistosity below the Main Kabyle Thrust: chlorite, white mica are present in the refolded schistosity, with late albite blastesis. × 40.

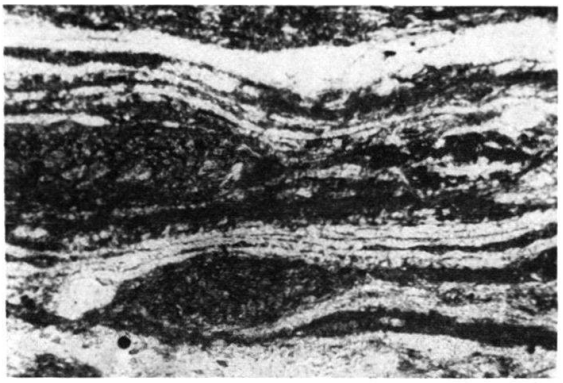

A

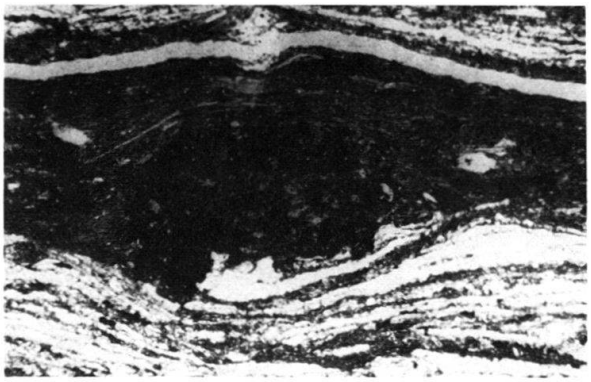

B

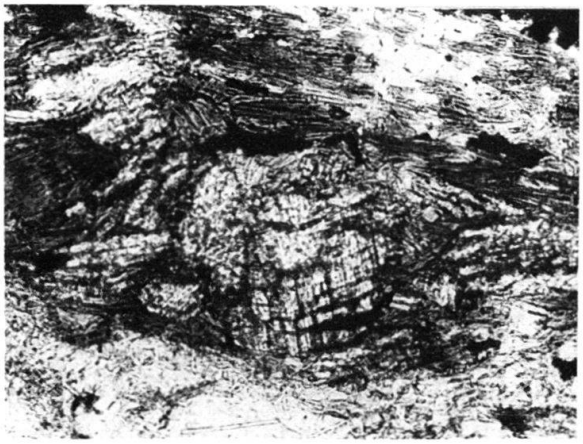

C

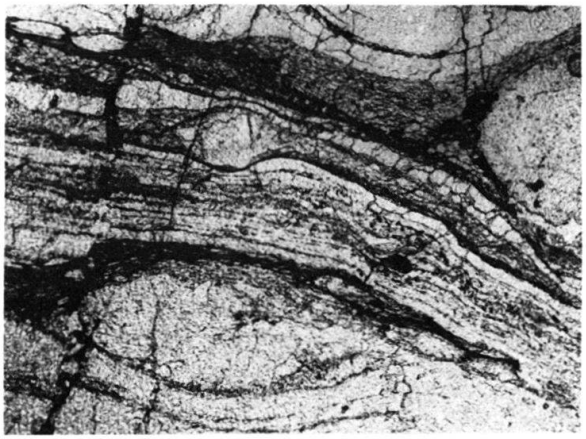

D

E

F

Plate 3

Fig. A — Apophyses of slightly deformed granite cutting hornfelses with andalusite. Note the small scale shear zones without penetrative deformation. Northern contact of the SAN granite (south to the left).

Fig. B — Foliated porphyritic granite, some 50 m south of Figure A.

Fig. C — Typical foliated granite of the central part of the massif. Note the elongation of the xenolith in a plane slightly oblique to the foliation plane coherent with a simple shear type deformation with a S–SE vergence.

Fig. D — Orthogneiss with highly flattened xenolith. Note the sigmoidal shape of feldspar clasts indicating a SE vergence and the associated microfolding of the foliation plane. Vertical joints are of post-Miocene age.

Fig. E — Mylonitic orthogneiss with bands of leucocratic ultramylonite derived from aplite. Some hundred meters from the root of the massif.

Fig. F — Phyllonitic micaschists with lensoid boudins of leucocratic mylonitic metaaplite.

A

B

C

D

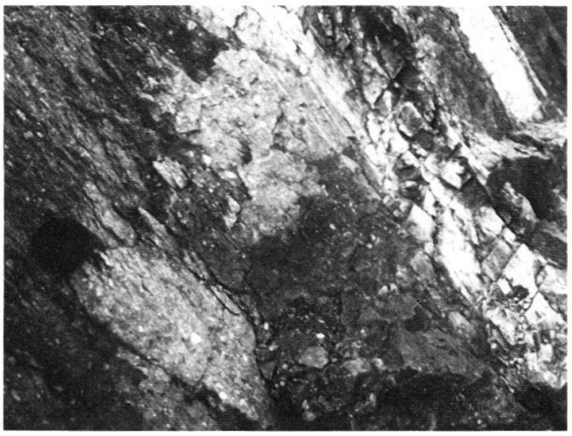

E

F